Vol. 36, No. 4 (2014) 406-418

Tribology in Industry

www.tribology.fink.rs

RESEARCH

Structural and Contact Analysis of a 3-Dimensional Disc-Pad Model with and without Thermal Effects

A. Belhocine[a], N.M. Ghazali[b], O.I. Abdullah[c]

[a]*Faculty of Mechanical Engineering, University of Sciences and the Technology of Oran, L.P 1505 El - MNAOUER, USTO 31000 ORAN, Algeria,*
[b]*Mechanical Engineering Dept., Faculty of Engineering, South Valley University, Qena-83523, Egypt,*
[c]*System Technology and Mechanical Design Methodology, Hamburg University of Technology, Germany.*

Keywords:

Finite element
Disc-pad model
Temperature
Deformation
Stress
Contact pressure

Corresponding author:

Ali Belhocine
Department of Mechanical Engineering, USTO Oran University
LP 1505 El-Maouer USTO 31000 Oran , Algeria
E-mail: al.belhocine@yahoo.fr

A B S T R A C T

The motivation of this work is to identify thermal effects on the structural and contact behaviour of a disc-pad assembly using a finite element approach. The first analysis is performed on the disc-pad model without the presence of thermal properties. Structural performance of the disc-pad model such as deformation and Von Mises stress is predicted. Next, thermomechanical analysis is performed on the same disc-pad model with the inclusion of convection, adiabatic and heat flux elements. The prediction results of temperature distribution, deformation, stress and contact pressure are presented. Comparison of the structural performance between the two analyses (mechanical and thermomechanical) is also made. From this study, it can assist brake engineers to choose a suitable analysis in order to critically evaluate structural and contact behaviour of the disc brake assembly.

1. INTRODUCTION

In basic working operation, a disc or drum brake system has to reduce wheel speed when a driver desires vehicle deceleration. The kinetic energy generated by a vehicle in terms of wheel speed is converted into heat energy due to the application of the brake system. The friction force between disc/drum and brake pad/brake shoe applies friction torque to the wheel in the opposite direction of the car's movement. This result in the reduction of vehicle speed and heat energy occurring in the brake disc/drum causes a temperature increment in the disc/drum swept area during the brake application. This physical action of the brake disc/drum causes heat conduction to the adjacent braking system components [1]. Lee [2] stated that inconsistent dissipation of heat inside the brake disc could cause deformation of the disc. Even worst, the disc deformation could also cause friction loss and consequently led to brake fade [3]. Furthermore, high temperatures of the brake disc could cause cracking in the brake disc material due to high thermal stresses. On top of that these factors also cause vibration [4, 5]. It is become common in the brake research

community to fully utilize finite element approach in order to identify and predict disc/drum brake structural performance. For instance, Koetniyom [6] performed temperature analysis on brake discs under heavy operating conditions. He found that the physical shape of vehicle brake discs play a significant role in determining the temperature characteristics including the overall brake efficiency. Kamnerdtong et al. [7] attempted to link the interaction between mechanical and thermal effects with disc movements and heat caused by frictions. They concluded that, from finite element analysis, temperatures on the disc surface changed at each point over the period, which indicates inconsistent dissipation and temperature differences in each side of the disc. Hence, inconsistent contact between disc and pad could affect material deformation.

Belhocine et al. [8] used the finite element Sofware ANSYS to study the thermal behaviour of the dry contact between the discs of brake pads at the time of braking phase. Temperature distribution obtained by the transient thermal analysis was used in the calculations of the stresses on disc surface. Abdullah and Schlattmann [9] used finite element method to to calculate the heat generated on the surfaces of friction clutch and temperature distribution for case of bands contact between flywheel and clutch disc, and between the clutch disc and pressure plate (one bad central and two bands) and compared with case of full contact between surfaces for single engagement and repeated engagements. In other work, Abdullah et al. [10] used the finite element method used to study the contact pressure and stresses during the full engagement period of the clutches using different contact algorithms. Moreover, sensitivity study for the contact pressure was presented to indicate the importance of the contact stiffness between contact surfaces.

Akhtar et al. [11] employed finite element (FE) method to explain the transient thermoelastic phenomena of a dry clutch system. The effect of sliding speed on contact pressure distribution, temperature and heat flux generated along the frictional surfaces was analyzed. Sowjanya and Suresh [12] conducted a static structural analysis of the disc brake whose some composite materials were selected to compare the results obtained such as deflection and stresses. In the research developed by Reddy et al.[13], thermal and structural coupled analysis was carried out to find the strength of the disc brake. Gnanesh et al. [14] investigated thermal-structural analysis of solid and vented disc brake disc using FE approach in the case of design with no holes and with holes in the disc. The materials used in the simulation were cast iron, stainless steel and aluminum metal matrix composites. Manjunath and Suresh [15] performed a structural and thermal analysis of the disc brake disc using FE method to determine the deformation and the Von Mises stress established in the disc for the both solid and ventilated discs with two different materials to enhance performance of the disc. In the work carried out by Parab et al. [16], structural and thermal analysis was carried out on the disc brakes using three materials i.e. stainless steel, cast iron and carbon-carbon composite. Structural analysis was done on the disc brake to assess strength of the disc brake, whilst thermal analysis was performed to analyze the thermal effect on the disc brake behavior. In research carried out by Tiwari et al. [17], a transient structural analysis of the disc of disc brake aimed to determine the variation of the stresses and deformation across the disc brake profile.

The aim of this paper was to investigate structural and contact behaviours of the brake disc and pads during the braking phase with and without thermal effects. Firstly, total deformation of the disc-pads model at the time of braking and the stress and contact distributions of the brake pads were determined. Later, results of the thermoelastic coupling such as Von Mises stress, contact pressure field and total deformations of the disc and pads were also presented which will be useful in the brake design process for the automobile industry.

2. FINITE ELEMENT (FE) MODEL

In this work, a three-dimensional FE model consists of a ventilated disc and two pads is employed as illustrated in Fig. 1. Whilst, Fig. 2 shows contact zone between the disc and pad. Details of the mesh properties are given in Table 1.

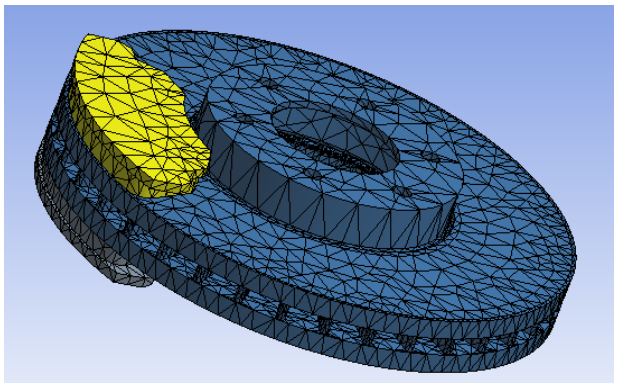

Fig. 1. FE model of a disc-pad assembly.

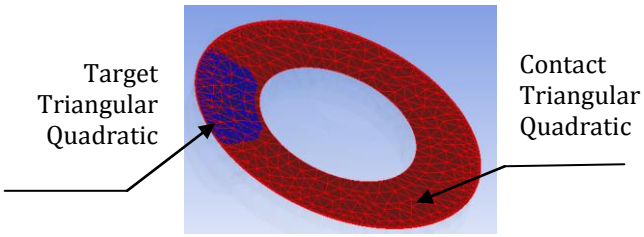

Fig. 2. Contact zone of the disc and pad.

Table 1. Finite element mesh properties.

Description	Nodes	Elements
Disc	34799	18268
Pad 1	1446	650
Pad 2	1461	660
Contact zone 1	0	914
Contact zone 2	0	83

The selected material of the disc is gray cast iron FG 15 with high carbon content and the brake pad has an isotropic elastic behavior whose mechanical characteristics of the two parts are provided in Table 2. Design parameters of the brake components are given in Table 3. A commercial FE software, namely ANSYS 11 (3D) is fully utilized to simulate structural deformation, stress, temperature and contact pressure distributions of the disc brake during braking application.

Table 2. Thermoelastic properties of the disc and pad.

	Disc	Pad
Young modulus E (GPa)	138	1
Poisson's ratio ν	0 ,28	0,25
Density ρ (kg/m³)	7250	1400
Coefficient of friction μ	0 ,2	0,2
Thermal conductivity,k (W/m°C)	57	5
Specific heat, c (J/Kg. °C)	460	1000

Table 3. Design parameters of the disc and pads.

	Disc	Pad
Volume (m³)	9,5689e-004	8,5534e-005
Surface (m²)	0 ,24237	1,8128 e-002
Mass (kg)	6,9375	0,44975
Inertia moment Ip1 (kg·m²)	3,5776e-002	2,7242e-005
Inertia moment Ip2 (kg·m²)	6,9597e-002	1,5131e-004
Inertia moment Ip3 (kg·m²)	3,5774e-002	1,2863e-004

2.1 Determination of hydraulic pressure

In this study, initial mechanical calculation aims at determining the value of the contact pressure (presumably constant) between the disc and the pad. It is supposed that 60% of the braking forces are supported by the front brakes (both discs), that is to say 30 % for a single disc [18]. The force of the disc for a typical vehicle is calculated using the vehicle data contained in Table 4, resulting in working forces to the brake disc:

$$F_{disc} = \frac{(30\%).\frac{1}{2}Mv_0^2}{2.\frac{R_{rotor}}{R_{tire}}\left(v_0.t_{stop} - \frac{1}{2}\left\{\frac{v_0}{t_{stop}}\right\}t_{stop}^2\right)} = 1047{,}36[N] \quad (1)$$

The rotational speed of the disc is calculated as follows:

$$\omega = \frac{v_0}{R_{tire}} = 157.89\ Rad/s \quad (2)$$

Total disc surface in contact with pads is 35797 mm² as depicted in Fig. 3.

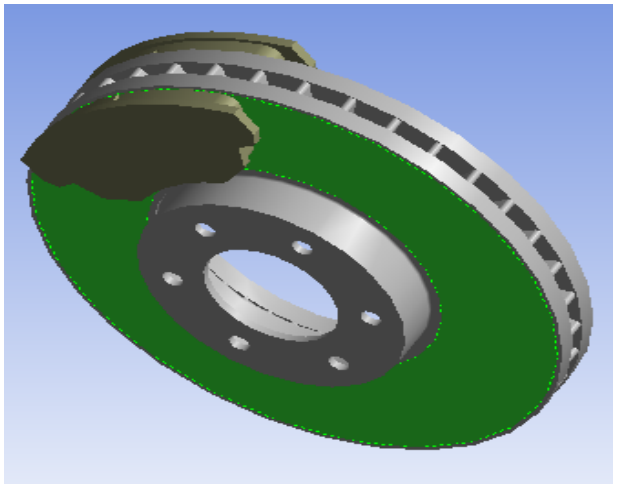

Fig. 3. Contact surface of the disc.

The hydraulic pressure is obtained using Eq. (3) [19]:

$$P = \frac{F_{disc}}{A_c.\mu} = 1\ [MPa]$$

Where A_c is the surface area of the pad in contact with the disc and μ is the friction coefficient. The surface area of the pad in contact with the disc in mm² is given directly in ANSYS by selecting this surface as indicated the green color in Fig. 4. In the case of a brake pad without groove, the calculation of the hydraulic pressure is obtained in the same manner.

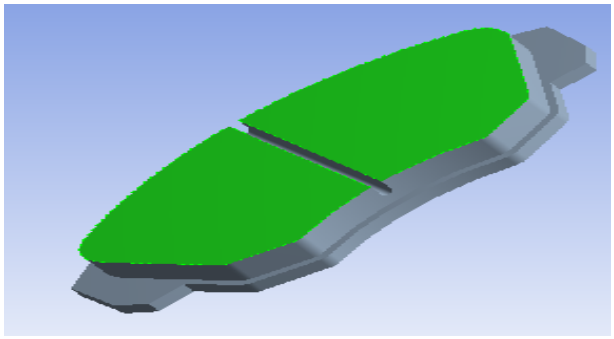

Fig. 4. Contact surface of the pad.

Table 4. Vehicle data.

Vehicle mass - M [kg]	1385
The initial velocity – v_0 [m/s]	60
Duration of braking application [s] - t_{stop}	45
The effective radius of the disc – [mm]	100.5
The radius of the wheel –[mm]	380
Friction coefficient disc/pad μ [/]	0.2
Pad Surface A_d [mm²]	5246.3

2.2 Boundary conditions and loading of the disc and pads

In this FE model, boundary conditions are imposed on the models (disc-pad) as shown in Fig. 5(a) for applied pressure on one side of the pad and Fig. 5(b) for applied pressure on both sides of the pad. The disc is rigidly constrained at the bolt holes in all directions except in its rotational direction. Meanwhile, the pad is fixed at the abutment in all degrees of freedom except in the normal direction to allow the pads move up and down and in contact with the disc surface [20].

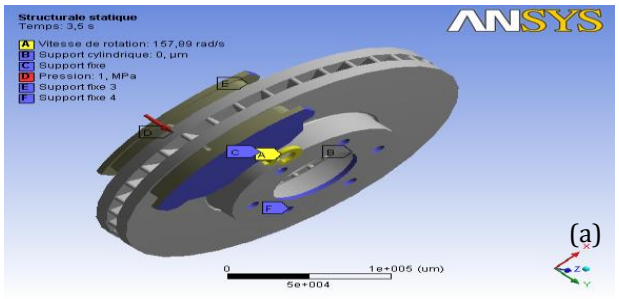

(a) One side

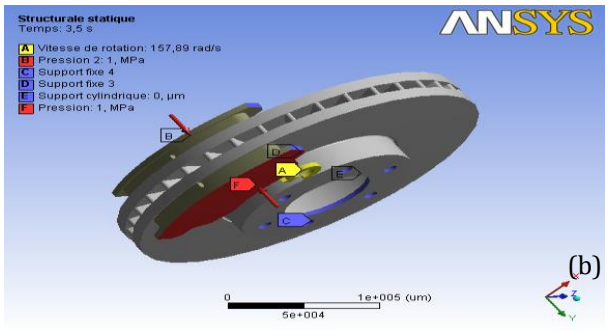

(b) Two sides

Fig. 5. Boundary conditions and loading imposed on the disc-pads.

2.3 Thermal boundary conditions

To express the heat transfer in the disc brake model, thermal boundary conditions and initial condition have to be defined. As shown in Fig. 6, at the interface between the disc and brake pads, heat is generated due to sliding friction, which is shown as dashed lines. In the exposed region of the disc and brake pads, it is assumed that heat is exchanged with the environment through convection [21]. Therefore, the convection surface boundary condition is applied there. On the surface of the back plate, adiabatic or insulated surface boundary condition is used and presented in Fig. 6.

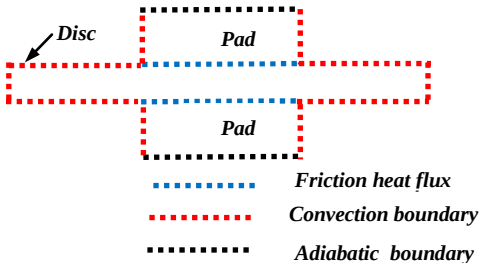

Fig. 6. Boundary condition for thermal analysis of the disc brake.

3. CONTACT ALGORITHM

There are three basic types of contacts used in ANSYS software, namely single contact, node-to-surface contact, and surface-to-surface contact. Surface-to-surface contact is the most common type of contact used for bodies that have arbitrary shapes with relatively large contact areas. This type of contact is most efficient for bodies that experience large values of relative sliding such as a block sliding on a plane or sphere sliding within groove [22]. Surface-to-surface contact is the type of contact assumed in this analysis because of the larger areas of clutch elements in contact. To model the frictional contact, the CONTA174 finite element is utilized. CONTA 174 is an 8-node element that is intended for general rigid-flexible and flexible-flexible contact analysis and is utilized to represent contact and sliding between 3-D surfaces. The element is applied to 3-D structural and coupled field contact analyses.

The contact element permits the use of both isotropic and orthotropic friction models. In this case, an isotropic friction model was used with a variable coefficient ranging between 0.35 and 0.55 and a starting value of 0.45 that correspond to the coupling materials which are determined experimentally. A uniform stick-slip behavior in all directions is also presumed. For the finite element CONTACT174, the rate of frictional dissipation is evaluated using the frictional heating factor and is given by:

$$q = FHTG\,\tau V$$

Where: τ is the equivalent frictional stress, V– the sliding rate and $FHTG$ – the fraction of frictional dissipated energy converted into heat (the default value of 1 was used for this parameter). The amount of frictional dissipation on contact and target surfaces is given by:

$$q_c = F_w F_f \tau V$$

$$q_T = (1 - F_w) F_f \tau V$$

Where q_c is the amount of frictional dissipation on the contact side, q_t – the amount of frictional dissipation on the target side and $FWGT$ is a weighted distribution factor (the default value of to 0.5 was used for this parameter). The relationships presented previously are valid only for the sliding mode of friction and a coefficient of friction greater than zero. To take into account the conductive heat transfer between contact and target surface, you need to specify the thermal contact conductance coefficient which is real constant TCC. The conductive heat transfer between two contacting surfaces is defined by:

$$q = TCC.(T_t - T_c)$$

Where q is the heat flux per area, TCC is the thermal contact conductance coefficient for force-based node for surface contact, T_t and T_c are the temperatures of the contact points on the target and contact surfaces. For surface-to-surface elements, ANSYS offer several different contact algorithms: Penalty method augmented Lagrangian, Lagrange multiplier on contact normal and penalty on tangent, pure Lagrange multiplier on contact normal and tangent, and internal multipoint constraint. In this work, a penalty method has been chosen. The penalty method uses a contact "spring" to establish a relationship between the two contact surfaces. The spring stiffness is called the contact stiffness (see Fig. 7). The contact force (pressure) between two contact bodies can be written as follows:

$$F_n = k_n x_p$$

Where F_n is the contact force, k_n is the contact stiffness, and x_p is the distance between two existing nodes, or separate contact bodies (penetration or gap).

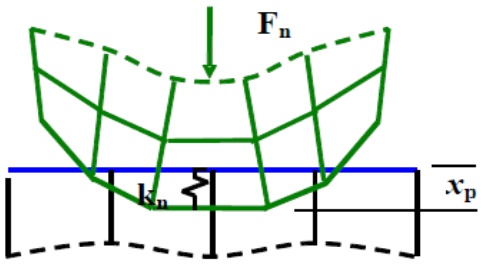

Fig. 7. The contact stiffness between the disc and pad.

The stiffness relationship between contact and target surfaces will decide the amount of the penetration. Higher values of contact stiffness will decrease the amount of penetration but can lead to ill conditioning of the global stiffness matrix and convergence difficulties. Lower values of contact stiffness can lead to a certain amount of penetration and low enough to facilitate the convergence of the solution. The contact stiffness for an element of area A is calculated using the following formula [23]:

$$F_{kn} = \int \{f_i\}(e)\{f_i\}^T dA$$

The default value of the contact stiffness factor (F_{KN}) is 1, and it is appropriate for bulk deformation. If bending deformation dominates the solution, a smaller value of F_{KN} = 0.1 is recommended.

4. FINITE ELEMENT RESULTS AND DISCUSSION

4.1 Disc-pad model without thermal effects

The computer code ANSYS also allows the determination and the visualization of structural deformations due to the sliding contact between the disc and the pads. The results of calculations of contact described in this section relate to displacements or the total deformation during the loading sequence, the field of equivalent Von Mises stress on the disc, the contact pressures of inner and outer pad at different braking period.

4.1.1. Disc-pad deformation

Figures 8(a) – 8(f) show disc deformations against braking time. It is noted that the large deformation is always found at the outer radius of the disc that is the area in contact with the pad. From the figures it can be seen that the highest deformation is 53 μm and it is predicted at braking time of t = 3.5s and onwards. As for the pads, the huge deformation is located at the outer radial region (visualized in the red colour) as depicted in Fig. 9. It is also seen that the pads are less deformed compared to the disc and this is shown in Fig. 10. At braking time of t= 3.5 s and onwards, the maximum deformation of the pads is predicted at 19 μm which is 64 % lower than that of the disc. This is due to structural stiffness and type of constraints that have been assigned to the disc and pads.

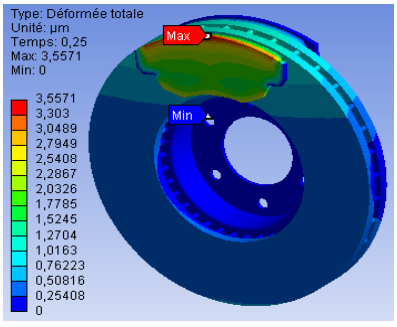

-a- *: at time t= 0,25 [s].*

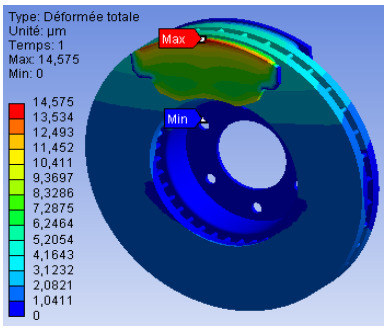

-b- *: at time t= 1 [s].*

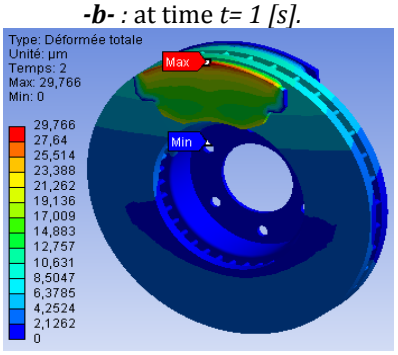

c- *: at time t= 2 [s].*

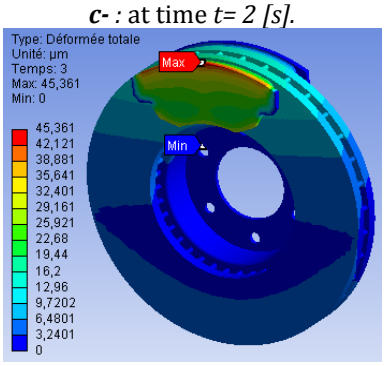

-d- *: at time t=3s*

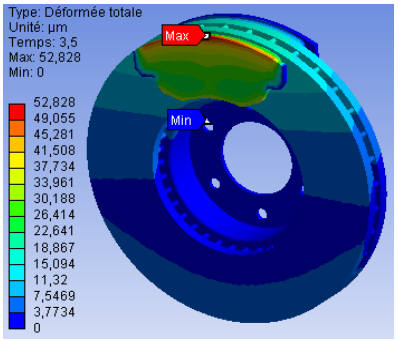

-e- *: at time t= 3.5s*

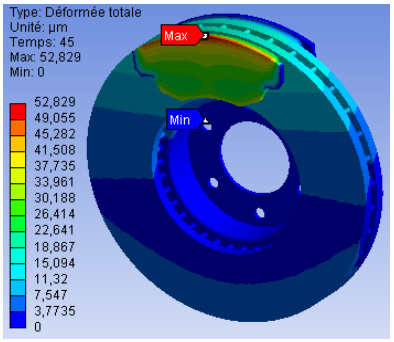

-f- *: at time t= 45s*

Fig. 8. Disc deformation at different braking time.

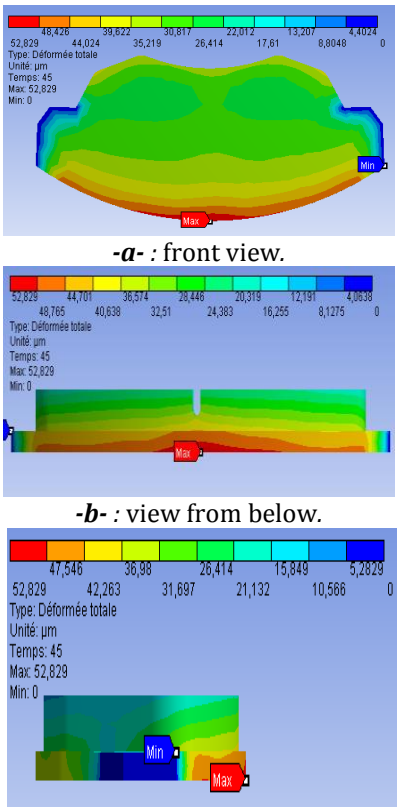

-a- *: front view.*

-b- *: view from below.*

-c- *: right view.*

Fig. 9. Pad deformation at braking time t = 45s.

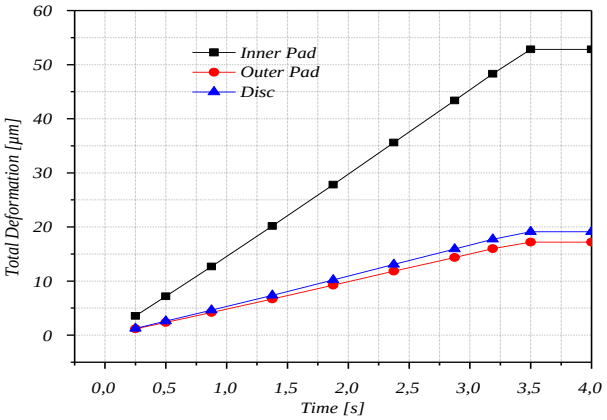

Fig. 10. Deformation of the disc and pads at different braking period

4.1.2. Stress distribution of the pad

From Figures 11(a)-11(h), it can be observed that the equivalent Von Mises stress is distributed almost symmetrically between the leading and trailing side of the pad. These stress distributions are barely unchanged over braking time except the stress value. It shows that the stress increases gradually and it reaches its maximum value of 5.3 MPa at braking time of 3.5 s and onwards. The highest stress is predicted on the left side and the outer radius of the pad whilst the lowest stress is located on the lower radius of the pad and near the groove area. Figure 12 shows a clear picture of stress distributions at braking time t = 45 s across the inner pad contact surface. It can be seen that more uniform stress distribution occur at the lower radius of the pad compared to the outer radius and center region of the pad. In addition, the highest stress is generated on the right and left side at the outer radius and the center region of the pad, respectively.

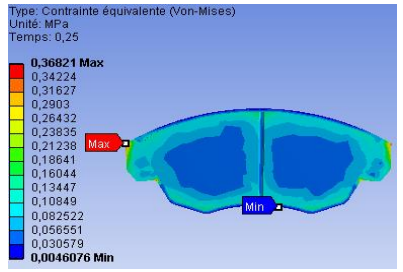

-a- *: at time t= 0,25 [s].*

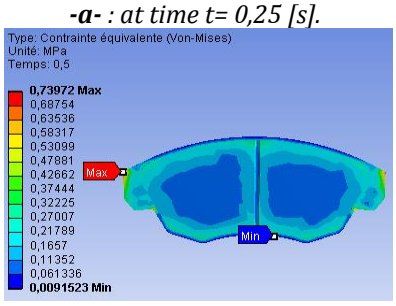

-b- *: at time t= 0,5 [s].*

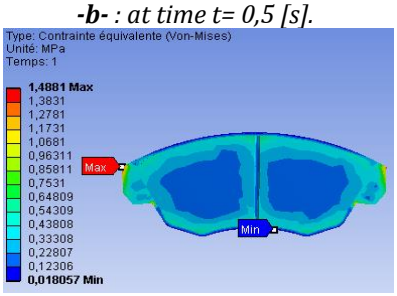

-c- *: at time t= 1 [s].*

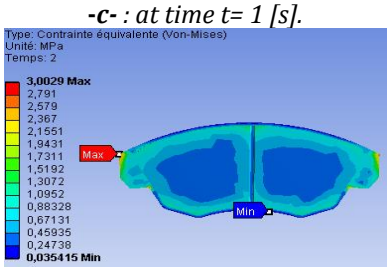

-d- *: at time t=2 [s].*

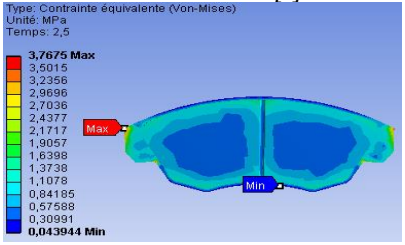

-e- *: at time t= 2,5 [s].*

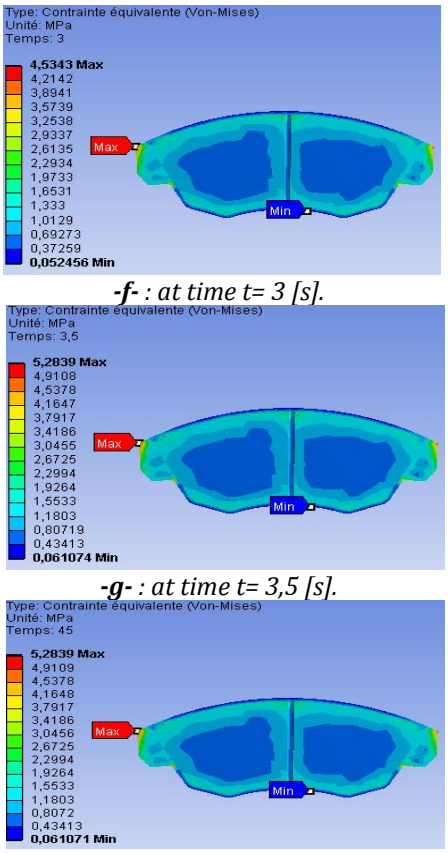

Fig. 11. Von Mises stress distribution of the pad over braking time.

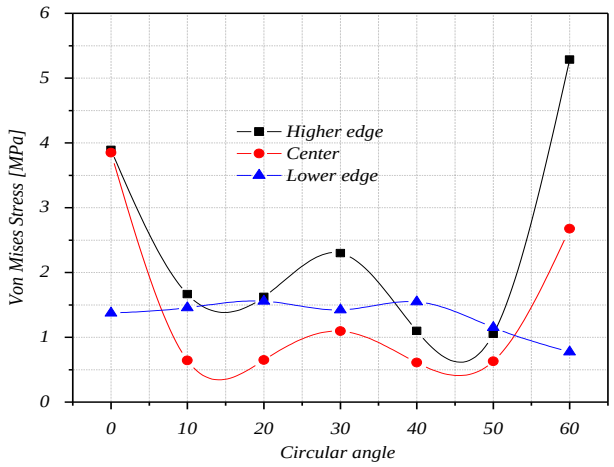

Fig. 12. Von Mises stress at different angular positions of the pad.

4.2 Disc-pad model with the thermal effect

In this section, structural and thermal analyses are coupled using ANSYS Multiphysics to identify the stress levels and global deformations of the model studied during the braking phase under the effect of temperature.

4.2.1. Temperature distribution

The initial temperature of the disc and pads is set at 20 °C, and the surface convection condition is applied to all surfaces of the disc and the convection coefficient of 5 W/m²°C is applied at the surface of the two pads. It shows in Fig. 13 that at braking time of 1.7s the disc and pad surface generates quite high temperature, i.e. 346 °C. However the upper part of the back plate shows a lower temperature approximately at 90 °C. This is caused by the effect of convection ambient air.

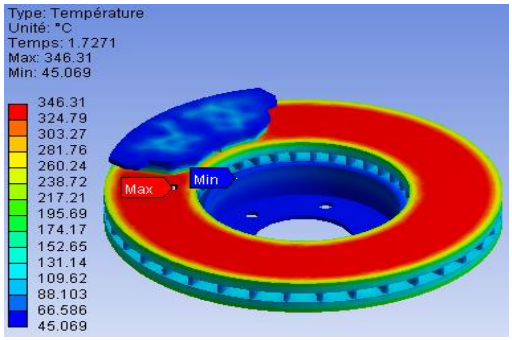

Fig. 13. Temperature distribution of the disc and pads at braking time t = 1.7s.

4.2.2. Deformation and Von Mises stress of the disc-pad model

In this coupled structural-thermal analysis, the aim is to gain a better understanding of the total deformation of the disc when it is not only subjected to the load from the pads but also the expansion induced by the effect of temperature. Figure 14 shows the disc deformations at the nodes located in the mean and outer radius of the disc.

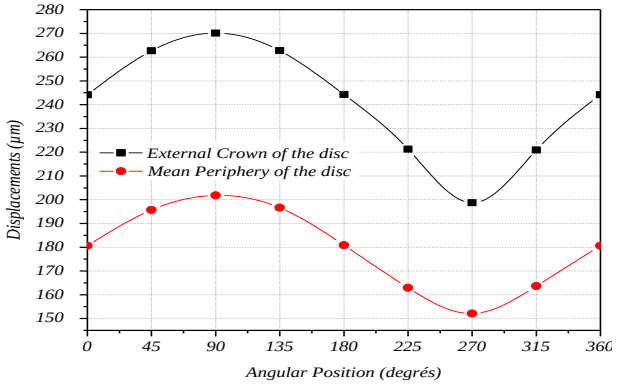

Fig. 14. Disc deformation at the mean and outer radius over angular positions at braking time t = 3.5 s.

A clear difference of the disc deformation can be found between these two regions where the outer radius of the disc is recording higher deformation than the mean radius. The curves indicate umbrella phenomenon which is resulting from the heating of non- parallel paths of friction with respect to the initial position. It is also observed that the disc deformation increases linearly as a function of the disc radius as showed in Fig. 15. The highest deformation is predicted at an angular position of 90° and the lowest deformation is located at 270°.

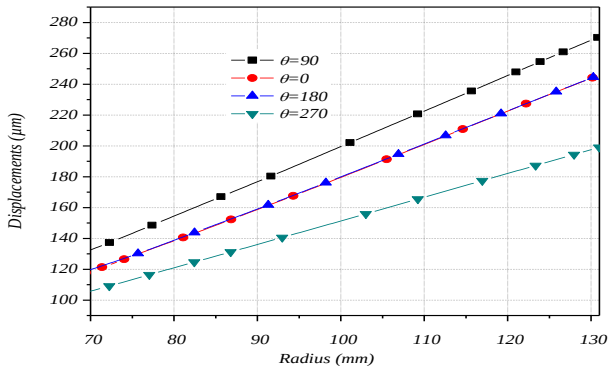

Fig. 15. Disc deformation at different radius and angular positions at braking time t = 3.5 s.

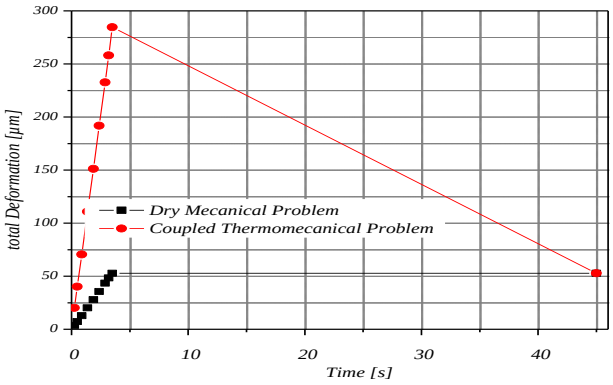

Fig. 16. Disc deformation with and without thermal effects.

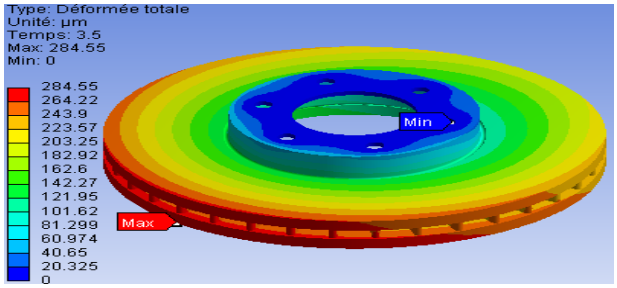

Fig. 17. Maximum total deformation of the disc with thermomechanical coupling.

The result shows that there are a significant difference between the mechanical and thermo-elastic model in terms deformation and contact pressure. From Fig. 16, it is shown that the disc deforms severely under the effect of temperature. For instance at the braking time of 3.5 s, the disc with the thermal effect deforms at 280 microns compared to 53 microns for the disc without the thermal effect. This clearly indicates that the temperature has a strong influence on the thermomechanical response of the brake disc. During a braking maneuver, the maximum temperature achieved on the tracks depends on the storage capacity of the thermal energy in the disc. It is observed in Fig. 17, that the maximum displacement is localized on the slopes of friction, the fins and the outer ring. This phenomenon is due to the fact that the deformation of the disc is caused by the heat (the umbrella effect) which can lead to cracking of the disc. In this case, the thermo- coupling analysis is quite important where thermal gradients and expansions generate thermal stresses in addition to the mechanical stress.

4.2.3. Von Mises stress at the inner pad

In this section, influence of the pad groove and the loading modes (single and dual piston) on the equivalent Von Mises stress distribution is presented. The stress evolution for three pad designs can be seen in Fig. 18(a)-18(g). It shows that at the beginning of braking time (t=1.7s) most of the pad contact surfaces are covered by a dark blue which indicates a lower stress. However, when it comes to braking time t = 45s the stress level has been increased where the colour spectrum now becomes almost an ocean blue. At this braking time, the stress distribution is also clearly noticed between those three pad designs. The presence of the groove and the double piston loading provide a positive effect on the stresses of the pad.

4.2.4. Contact pressure distribution

Contact pressure distribution that is being plotted in Fig. 19 is based on braking time *t* = 1.7s where the pad surface temperature is T = 346 ° C. It is seen that the contact pressure curves are almost identical in shape for three different regions of the pad. At 30° angle, contact pressure is predicted higher at the lower pad radius followed by the outer pad radius and middle pad radius. The most significant outcome is to see the effect of temperature on contact

pressure of the disc-pad model. From Fig. 20, one can observe the significant variation of the two curves. It is observed that the contact pressure distribution of the pads increase in a notable way, when the thermal and mechanical aspects are coupled. This gives an indication to the brake engineers that in order to evaluate brake performance thermomechanical analysis should be performed in the first place so that a realistic prediction can be achieved.

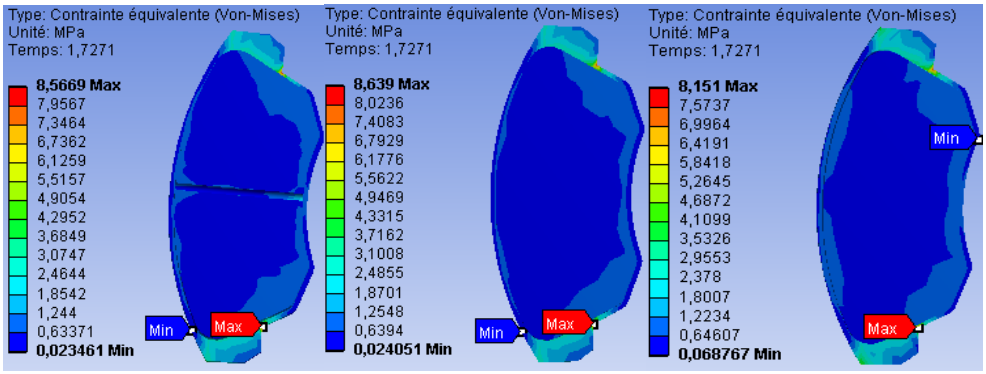

-a- *:* at time *t= 1.7s*

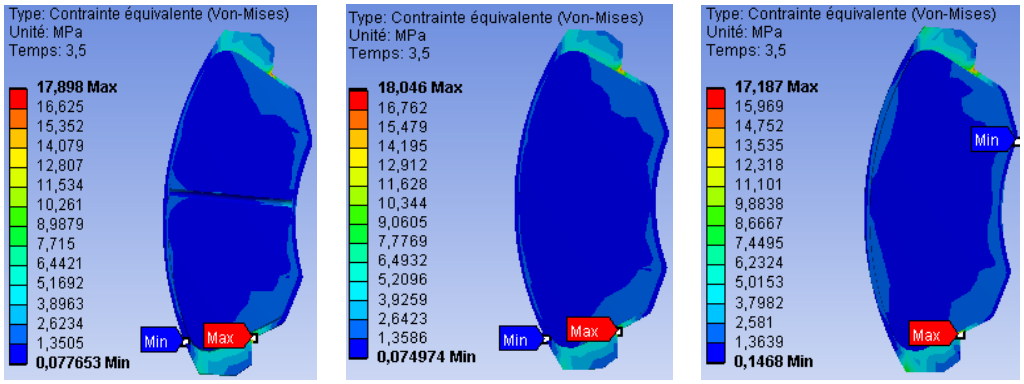

-b- *:* at time *t= 3.5s*

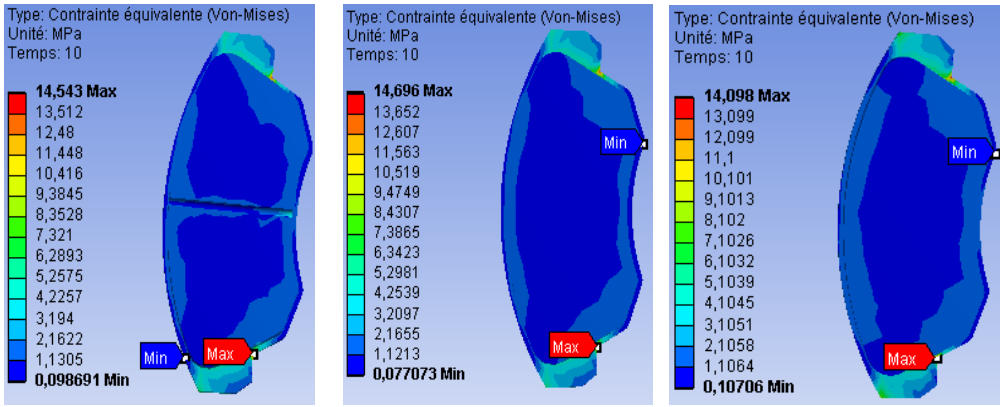

-c- *:* at time *t= 10s*

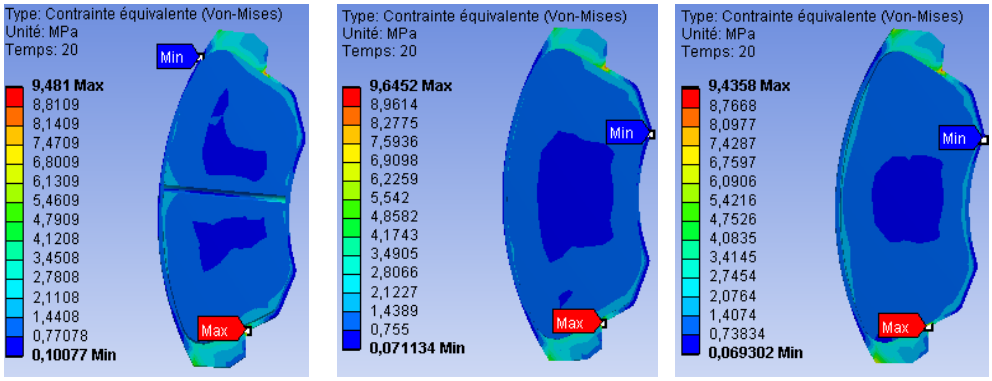

-d- *:* at time *t= 20s*

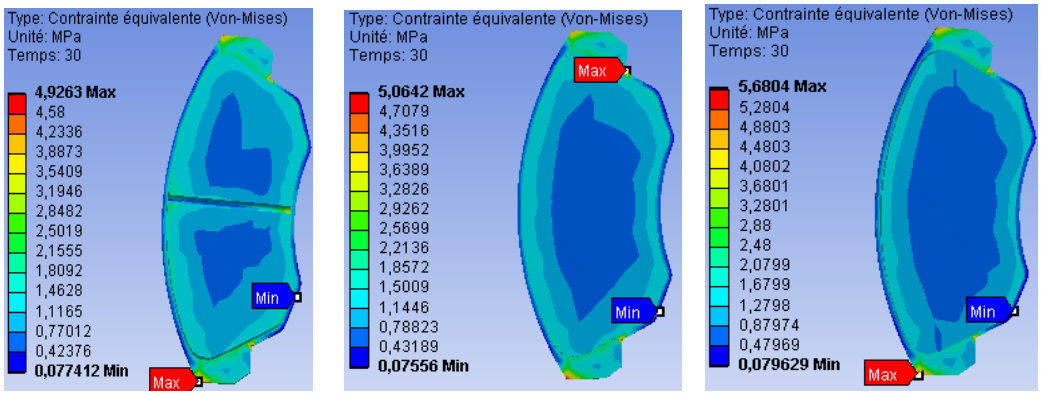

-e- *: at time t= 30s*

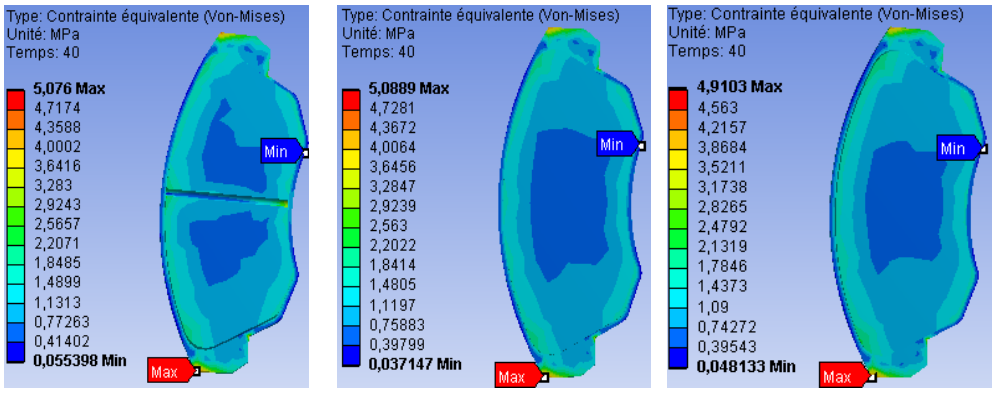

-f- *: at time t= 40s*

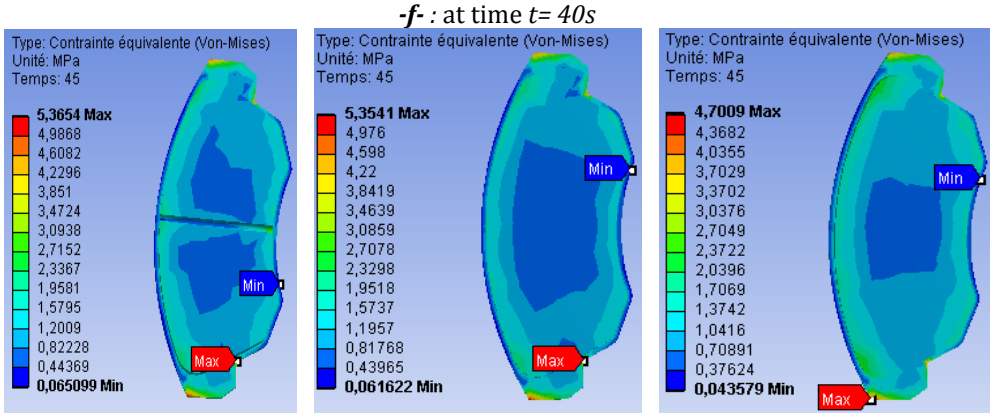

-g- *: at time t= 45s*

Fig.18. Distribution of von Mises stress at different braking time: Single piston with pad center-groove (left), Single piston without groove (center) and Double piston without pad groove (right).

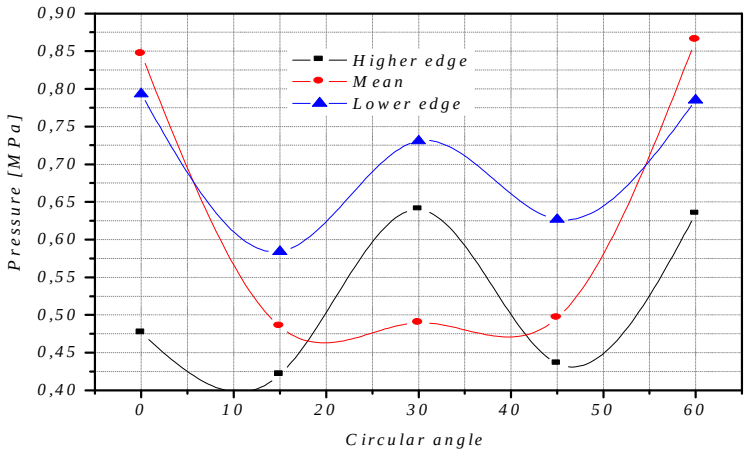

Fig. 19. Distribution of contact pressure along the lower, middle and upper radius of the pad at time t = 1.7 s.

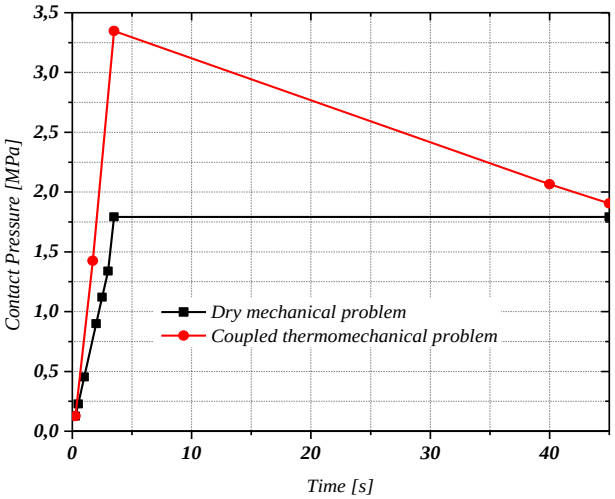

Fig. 20. Contact pressure of the inner pad.

5. CONCLUSION

In this work, a disc-pad model has been analysed using two approaches, namely mechanical and thermomechanical analysis. In addition to this, three pad designs are also simulated to identify its influence on the stress distribution. From the prediction results, it can be deduced that:

- Large deformation is occurred at the outer radius of the disc
- More uniform stress distribution is noticed for the pad without groove and with a double-piston loading
- Temperature has a significant effect on the structural and contact behaviour of the disc brake assembly. Large deformation and high contact pressure is found in the disc-pad model with the thermal effect

REFERENCES

[1] S. Lakkam, K. Suwantaroj, P. Puangcharoenchai, P. Mongkonlerdmanee, S. Koetniyom: *Study of heat transfer on front– and back-vented brake discs,* Songklanakarin J. Sci. Technol. Vol. 35, No. 6, pp. 671-681, 2013.

[2] K. Lee: *Numerical Prediction of Brake Fluid Temperature Rise During Braking and Heat Soaking*, The Soceity of Automotive Engineer Technical Paper, 1999-01-0483, pp. 1-9, 1999.

[3] G. Cueva, A. Sinatora, W.L. Guesser, A.P. Tschiptschin: *Wear Resistance of Cast Irons Used in Brake Disc rotors*, Wear, Vol. 255, No. 7, pp. 1256–1260, 2013.

[4] F. Bergman, M. Eriksson, S. Jacobson: *Influence of Disc Topography on Generation of Brake Squeal*. Wear, Vol. 225–229, No. 1, pp. 621–628, 1999.

[5] A. Papinniemia, C.S. Laia Joseph, J. Zhaob, L. Loader: *Brake squeal: a literature review*, Applied Acoustics, Vol. 63, No. 4, pp. 391–400, 2002.

[6] S. Koetniyom: *Temperature Analysis of Automotive Brake Discs,* The Journal of King Mongkut's University of Technology North Bangkok, Vol. 13, pp. 36-42, 2003.

[7] T. Kamnerdtong, S. Chutima, A. Siriwattanpolkul: *Analysis of Temperature Distribution on Brake Disc,* in: *Proceeding of the 19th ME-NETT*, October 19-21, 2005, Phuket, Thailand.

[8] A. Belhocine, A.R. Abu Bakar, M. Bouchetara: *Numerical Modeling of Disc Brake System in Frictional Contact,* Tribology in Industry, Vol. 36, No. 1, pp. 49-66, 2014.

[9] O.I. Abdullah, J. Schlattmann: *Effect of Band Contact on the Temperature Distribution for Dry Friction Clutch*, Tribology in Industry, Vol. 35, No. 4, pp. 317-329, 2013.

[10] O.I. Abdullah, J. Schlattmann, A.M. Al-Shabibi: *Stresses and Deformations Analysis of a Dry Friction Clutch System*, Tribology in Industry, Vol. 35, No. 2, pp. 155-162, 2013.

[11] M.M.J. Akhtar, I.O. Abdullah, J. Schlattmann: *Transient Thermoelastic Analysis of Dry Clutch System,* Machine Design, Vol. 5, No. 4, pp. 141-150, 2013.

[12] K. Sowjanya, S. Suresh: *Structural Analysis of Disc Brake Rotor,* International Journal of Computer Trends and Technology (IJCTT), Vol. 4, No. 7, pp. 2295-2298, 2013.

[13] V.C. Reddy, M.G. Reddy, G.H. Gowd: *Modeling And Analysis of FSAE Car Disc Brake Using FEM*, International Journal of Emerging Technology and Advanced Engineering, Vol. 3, No. 9, pp. 383-389, 2013.

[14] P. Gnanesh, C. Naresh, S.A. Hussain: *Finite element analysis of normal and vented disc brake rotor,* Int. J. Mech. Eng. & Rob. Res., Vol. 3, No. 1, pp. 27-33, 2014.

[15] TV. Manjunath, P.M. Suresh: *Structural and Thermal Analysis of Rotor Disc of Disc Brake*, International Journal of Innovative Research in Science, Vol. 2, No. 12, pp. 7741-7749, 2013.

[16] V. Parab, K. Naik, A.D. Dhale: *Structural and Thermal Analysis of Brake Disc,* International Journal of Engineering Development and Research, Vol. 2, No. 2, pp. 1398-1403, 2014.

[17] A.K. Tiwari, P. Yadav, H.S. Yadav, S.B. Lal: *Finite Element Analysis of Disc Brake by ANSYS Workbench*', International Journal of Research in Engineering & Advanced Technology, Vol. 2, No. 2, pp. 1-6, 2014.

[18] T. Mackin, S.C. Noe, K.J. Ball, B.C. Bedell, D.P. Bim-Merle, M.C. Bingaman, D.M. Bomleny, G.J. Chemlir, D.B. Clayton, H.A. Evans: *Thermal cracking in disc brakes*, Eng. Failure Analysis, Vol. 9, No. 1, pp. 63-76, 2002.

[19] G. Oder, M. Reibenschuh, T. Lerher, M. Šraml, B. Šamec, I. Poetry: *Thermal and stress analysis of brake discs in railway vehicules*, Advanced Engineering, Vol. 3, No. 1, pp. 95-102, 2009.

[20] N. Coudeyras: *Non-linear analysis of multiple instabilities to the rubbing interfaces:application to the squealing of brake* " PhD Thesis , Central school of Lyon-speciality: mechanics, December, 2009.

[21] S.B. Sarip: Lightweight *friction brakes for a road vehicle with regenerative braking*," Ph.D. Thesis, Engineering, Design and Technology, Bradford University, 2011.

[22] O.I. Abdullah, J. Schlattmann: *Contact Analysis of a Dry Friction Clutch System*, ISRN Mechanical Engineering, Vol. 2013, pp. 1-9, 2013.

[23] G.A. Mohr: *Contact stiffness matrix for finite element problems involving external elastic restraint*, Computers and Structures, Vol. 12, No. 2, pp. 189–191, 1980.